Chapter 3

Applications and numerical examples

This chapter presents an analysis of the results obtained solving the Stokes problem in both two and three dimensions. For each case two problems have been studied. The first one has an analytical solution in order to compare the accuracy of the numerical solution. The second one is the called cavity flow problem, a benchmark flow problem with determined boundary conditions.

3.1 Bidimensional case

The application of the proposed finite element formulation in two dimensions implies certain type of elements, shape functions and Gauss points and weights. They are displayed in figures 3.1 to 3.4. In particular, the elements used in this work are quadrilateral and triangular as can be seen in figure 3.1. The node numeration for each type of element is shown at figure 3.2. The integrals are calculated using a Gauss quadrature. The Gauss points coordinates and their corresponding weights are displayed in figure 3.3. Finally, the shape functions are listed in figure 3.4.

Mixed elements			
Figure	Name	Velocity interpolation	Pressure interpolation
	Q1Q0	Linear	Constant
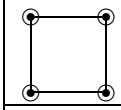	Q1Q1	Linear	Linear
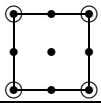	Q2Q1	Quadratic	Linear
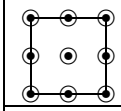	Q2Q2	Quadratic	Quadratic
	P1P0	Linear	Constant
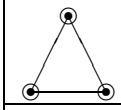	P1P1	Linear	Linear
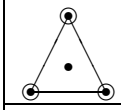	Mini	Linear	Linear
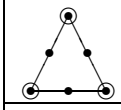	P2P1	Quadratic	Linear
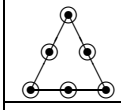	P2P2	Quadratic	Quadratic
• Velocity node ○ Pressure node			

Figure 3.1: Types of mixed elements in 2 dimensions

Node numeration	Type of element
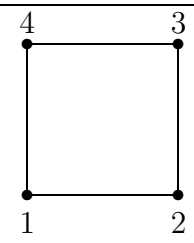	Linear Quadrilateral
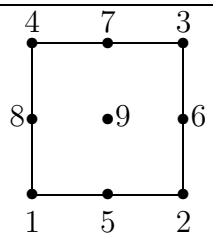	Quadratic Quadrilateral
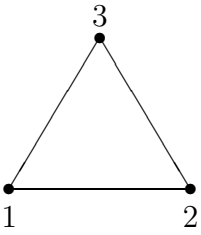	Linear Triangular
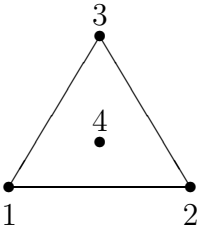	Linear Triangular (Mini)
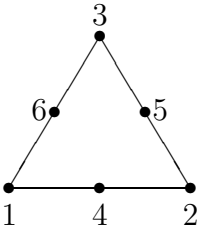	Quadratic Triangular

Figure 3.2: Node numeration in 2D elements

Element type	Approximation	Gauss points	Gauss weights
Quadrilateral	Linear	(.577350,.577350)	1.000000
		(.577350,-.577350)	1.000000
		(-.577350,.577350)	1.000000
		(-.577350,-.577350)	1.000000
	Quadratic	(-.774597,-.774597)	-.308642
		(0,-.774597)	.493827
		(.774597,-.774597)	.308642
		(-.774597,0)	.493827
		(0,0)	.790123
		(.774597,0)	.493827
		(-.774597,.774597)	.308642
		(0,.774597)	.493827
		(.774597,.774597)	.308642
Triangular	Linear	(.500000,.500000)	.166667
		(0,.500000)	.166667
		(.500000,0)	.166667
	Linear (Mini)	(.101286,.101286)	.062970
		(.101286,.797427)	.062970
		(.797427,.101286)	.062970
		(.470142,.470142)	.066197
		(.059716,.470142)	.066197
		(.470142,.059716)	.066197
		(.333333,.333333)	.112500
	Quadratic	(.333333,.333333)	-.281250
		(.600000,.200000)	.260417
		(.200000,.600000)	.260417
		(.200000,.200000)	.260417

Figure 3.3: Gauss Quadrature in 2 dimensions

Element type	Approximation	Shape functions
Quadrilateral	Constant	N_1=1
	Linear	N_1=$\frac{1}{4}(1-\xi)(1-\eta)$ N_2=$\frac{1}{4}(1+\xi)(1-\eta)$ N_3=$\frac{1}{4}(1+\xi)(1+\eta)$ N_4=$\frac{1}{4}(1-\xi)(1+\eta)$
	Quadratic	N_1=$\frac{1}{4}\xi(\xi-1)\eta(\eta-1)$ N_2=$\frac{1}{4}\xi(\xi+1)\eta(\eta-1)$ N_3=$\frac{1}{4}\xi(\xi+1)\eta(\eta+1)$ N_4=$\frac{1}{4}\xi(\xi-1)\eta(\eta+1)$ N_5=$\frac{1}{2}(1-\xi^2)\eta(\eta-1)$ N_6=$\frac{1}{2}\xi(\xi+1)(1-\eta^2)$ N_7=$\frac{1}{2}(1-\xi^2)\eta(\eta+1)$ N_8=$\frac{1}{2}\xi(\xi-1)(1-\eta^2)$ N_9=$(1-\xi^2)(1-\eta^2)$
Triangular	Constant	N_1=1
	Linear	N_1=ξ N_2=η N_3=$1-\xi-\eta$
	Linear (Mini)	N_1=ξ N_2=η N_3=$1-\xi-\eta$ N_4=$27\xi\eta(1-\xi-\eta)$
	Quadratic	N_1=$\xi(2\xi-1)$ N_2=$\eta(2\eta-1)$ N_3=$(1-2\xi-2\eta)(1-\xi-\eta)$ N_4=$4\xi\eta$ N_5=$4\eta(1-\xi-\eta)$ N_6=$4\xi(1-\xi-\eta)$

Figure 3.4: Shape functions in 2 dimensions

3.1.1 Problem with analytical solution

There are several Stokes problems (2.14) that have an analytical solution. These problems allows the validation of the numerical methods used to approximate the solution. In order to obtain an analytical solution, the main issue is to find a velocity field such as $\boldsymbol{\nabla v} = 0$. A proposed velocity field that follows that condition in two dimensions can be written as,

$$\begin{aligned} v_1(x,y) &= x^2(1-x)^2(2y-6y^2+4y^3) \\ v_2(x,y) &= -y^2(1-y)^2(2x-6x^2+4x^3) \end{aligned}$$

In addition, the viscosity is taken as $\nu = 1$. The pressure field can be chosen randomly because it is just needed its gradient. In this case, it has been chosen as,

$$p(x,y) = x(1-x)$$

Then, according to equation (2.12), the body forces verify

$$\begin{aligned} b_1 &= -\big[(24y-12)(x^4-2x^3+x^2)+(4y^3-6y^2+2y)(12x^2-12x+2)\big] \\ &\quad +1-2x \\ b_2 &= (24x-12)(y^4-2y^3+y^2)+(4x^3-6x^2+2x)(12y^2-12y+2) \end{aligned}$$

The problem is solved in a square domain of unity sides, $\Omega = [0,1]\times[0,1]$. This domain can be discretized in several ways depending on the finite elements used. In this work, the type of elements implemented are quadrilateral and triangular. Moreover, the discretization can be uniform or non-uniform distributed. Figure 3.5 shows an example of the different possible combinations implemented in this work. Figures 3.5(a) and 3.5(b) are a representation of 10x10 quadrilateral elements uniform and non-uniform distributed meshes. Similarly, figures 3.5(c) and 3.5(d) show 10x10 triangular uniform and non-uniform distributed meshes. It is important to note that for meshes of triangular elements, the elements located in the upper-right and lower-left corners are modified in order to avoid the three nodes located on the boundary.

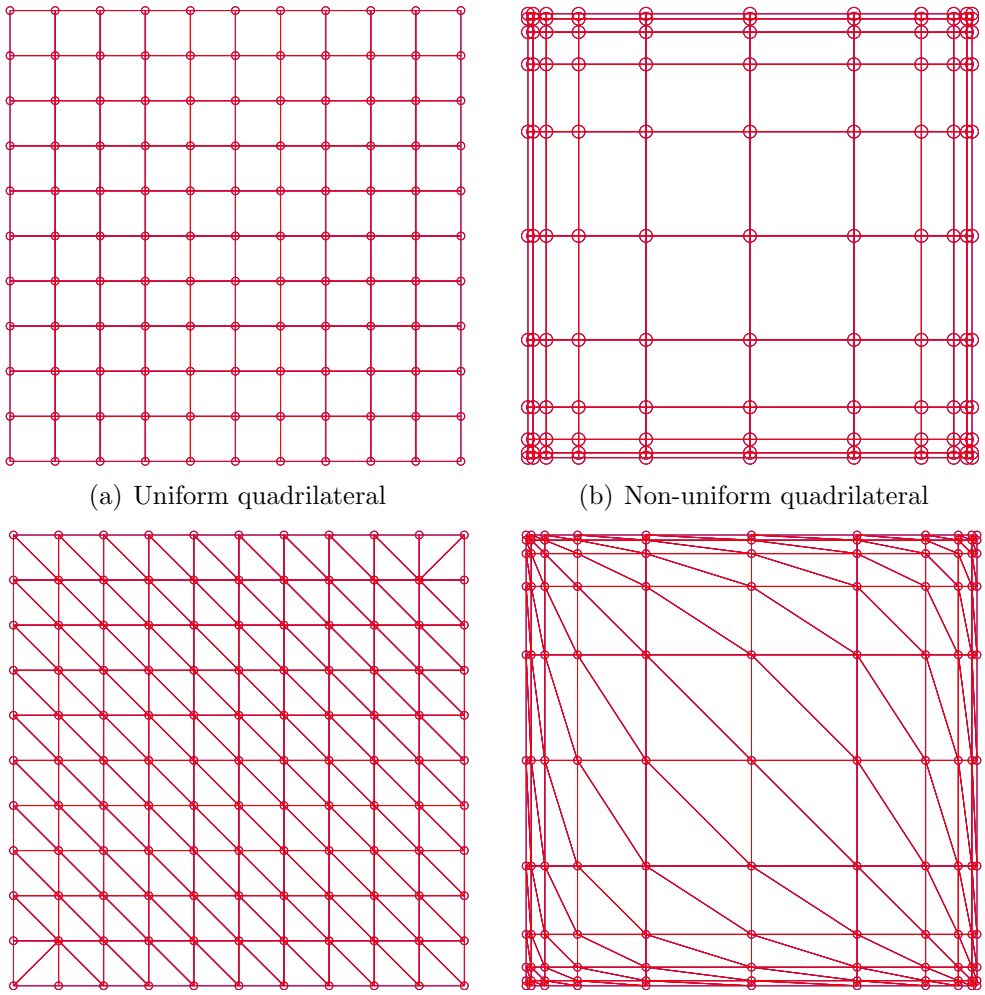

(a) Uniform quadrilateral

(b) Non-uniform quadrilateral

(c) Uniform triangular

(d) Non-uniform triangular

Figure 3.5: Type of 2D meshes

Comparison between stabilized and non-stabilized solution

In this section it is presented a serie of graphics comparing the stabilized and non-stabilized solution of this problem with the analytical solution. In all cases, the stationary Stokes problem has been solved using a mesh with 20x20 elements with an uniform distribution. On one hand, figure 3.6 shows the velocity and pressure fields for the analytical and the numerical non-stabilized solution. Note that the numerical solution, for both the pressure and velocity fields, is unacceptable due to the instabilities appeared. On the other hand, figure 3.7 displays the comparison between the analytical and the numerical stabilized solution. In this case, smooth and stable velocity and pressure fields are obtained. Therefore, the numerical solution is acceptable.

The solution of the problem using non-uniform distributed quadrilateral and triangular meshes leads to the same behavior as using uniform distributed meshes. In this particular case, the geometrical distribution of the elements does not affect the accuracy of the solution.

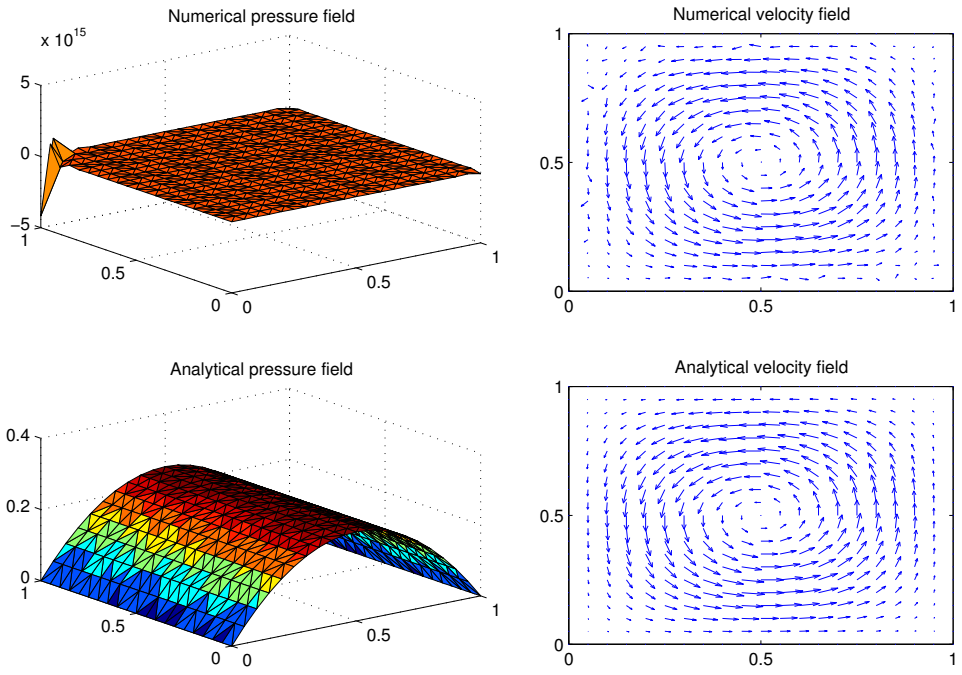

(a) Pressure field (b) Velocity field

Figure 3.6: Non-stabilized solution

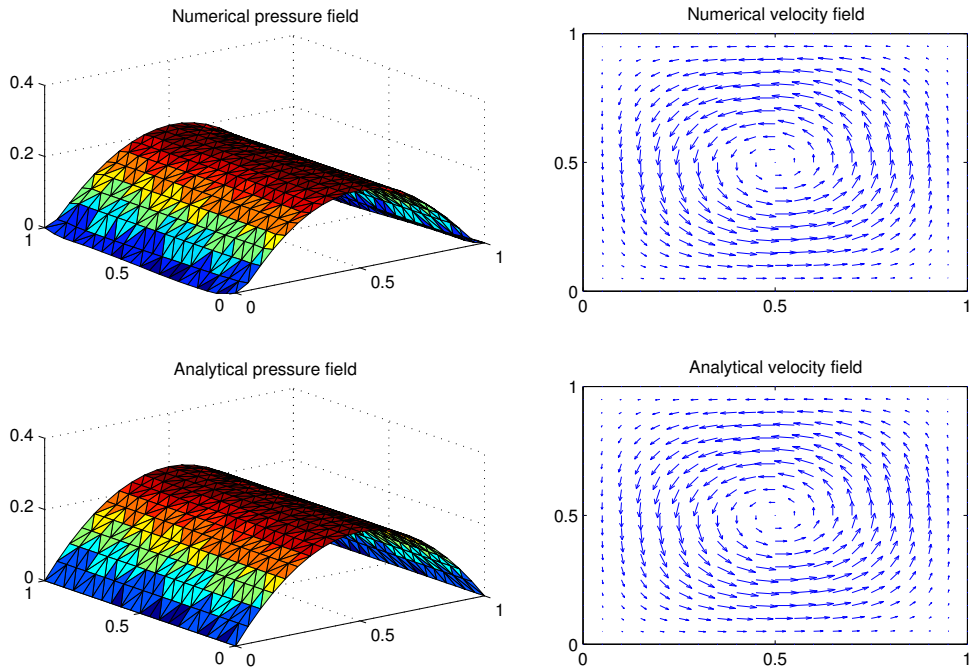

(a) Pressure field (b) Velocity field

Figure 3.7: Stabilized solution

Error depending on mesh size

The calibration of the efficiency of this stabilization method is made measuring the error between the numerical approximation and the analytical solution. The error has been calculated as an absolute error:

$$||\epsilon_v|| = ||\boldsymbol{v}_{num} - \boldsymbol{v}_{analyt}||_\infty \tag{3.1}$$

$$||\epsilon_p|| = ||p_{num} - p_{analyt}||_\infty \tag{3.2}$$

Figure 3.8 shows the maximum absolute error value for both stabilized linear element approximations in an uniform distributed mesh. That is, the linear quadrilateral and the linear triangular.

	Linear quadrilateral (Q1Q1)		Linear triangular (P1P1)	
N. of elements	Velocity Error	Pressure Error	Velocity Error	Pressure Error
20x20	$3.37{\cdot}10^{-4}$	$3.78{\cdot}10^{-2}$	$3.92{\cdot}10^{-4}$	$3.71{\cdot}10^{-2}$
25x25	$2.19{\cdot}10^{-4}$	$3.08{\cdot}10^{-2}$	$2.55{\cdot}10^{-4}$	$2.96{\cdot}10^{-2}$
30x30	$1.54{\cdot}10^{-4}$	$2.59{\cdot}10^{-2}$	$1.79{\cdot}10^{-4}$	$2.46{\cdot}10^{-2}$
35x35	$1.14{\cdot}10^{-4}$	$2.24{\cdot}10^{-2}$	$1.32{\cdot}10^{-4}$	$2.11{\cdot}10^{-2}$
40x40	$8.80{\cdot}10^{-5}$	$1.98{\cdot}10^{-2}$	$1.02{\cdot}10^{-4}$	$1.85{\cdot}10^{-2}$
45x45	$6.90{\cdot}10^{-5}$	$1.77{\cdot}10^{-2}$	$8.10{\cdot}10^{-5}$	$1.64{\cdot}10^{-2}$

Figure 3.8: Error of the stabilized solution in the analytical case.

Figure 3.9 shows the error plots obtained solving several stationary Stokes problems using uniform meshes composed by linear elements. In particular, the error of the velocity and pressure fields are plotted versus the element size in a log-log scale. The slopes obtained are shown in figure 3.10. The different values are separated by the type of element used (quadrilateral or triangular) and the error for the velocity and the pressure fields. Note that the velocity error is quadratic whereas the error in pressure is linear. These error properties correspond with what could be expected from the theory.

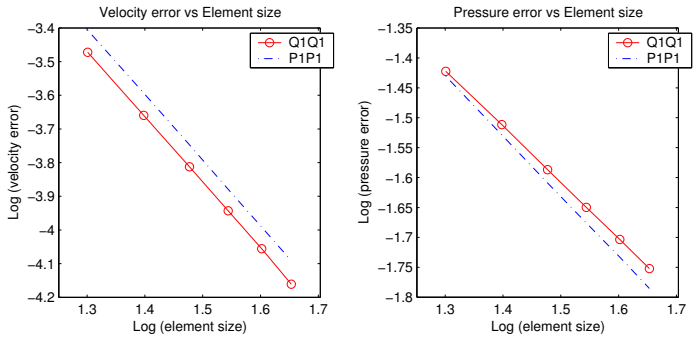

Figure 3.9: Error vs Element size.

	Linear quadrilateral	Linear triangular
Velocity error	1.996549	1.974577
Pressure error	1.005027	0.936629

Figure 3.10: Slope of the errors versus element size in logarithmic scale.

Analysis of the stabilization parameter

The stabilization parameter implemented in the Galerkin - Least Squares method depends basically on the element size, see equation (2.54). Note that the element size can be measured according to several criteria. Thus, depending on the selected measure, the accuracy of the method is different. Figure 3.11 shows the velocity and the pressure error obtained according to the definition of the element size. Note that there are some values not shown in the table. The reason is that those element measures are not possible to implement in triangular elements.

20x20 element uniform mesh	Velocity error		Pressure error	
	Q1Q1	P1P1	Q1Q1	P1P1
Side arithmetic mean	$5.6{\cdot}10^{-4}$	$7.8{\cdot}10^{-4}$	$1.5{\cdot}10^{-2}$	$2.1{\cdot}10^{-2}$
Maximum side	$9.4{\cdot}10^{-4}$	$1.2{\cdot}10^{-3}$	$2.9{\cdot}10^{-2}$	$2.7{\cdot}10^{-2}$
Minimum side	$4.5{\cdot}10^{-4}$	$4.9{\cdot}10^{-4}$	$0.7{\cdot}10^{-2}$	$1.0{\cdot}10^{-2}$
Side geometric mean	$5.3{\cdot}10^{-4}$	$7.2{\cdot}10^{-4}$	$0.6{\cdot}10^{-2}$	$1.2{\cdot}10^{-2}$
Diagonal arithmetic mean	$9.2{\cdot}10^{-4}$	-	$3.4{\cdot}10^{-2}$	-
Maximum diagonal	$9.2{\cdot}10^{-4}$	-	$3.4{\cdot}10^{-2}$	-
Minimum diagonal	$9.2{\cdot}10^{-4}$	-	$3.4{\cdot}10^{-2}$	-

40x40 element uniform mesh	Velocity error		Pressure error	
	Q1Q1	P1P1	Q1Q1	P1P1
Side arithmetic mean	$1.4{\cdot}10^{-4}$	$1.9{\cdot}10^{-4}$	$0.8{\cdot}10^{-2}$	$1.1{\cdot}10^{-2}$
Maximum side	$2.8{\cdot}10^{-4}$	$3.1{\cdot}10^{-4}$	$1.6{\cdot}10^{-2}$	$1.5{\cdot}10^{-2}$
Minimum side	$1.1{\cdot}10^{-4}$	$1.2{\cdot}10^{-4}$	$0.2{\cdot}10^{-2}$	$0.3{\cdot}10^{-2}$
Side geometric mean	$1.4{\cdot}10^{-4}$	$1.8{\cdot}10^{-4}$	$0.2{\cdot}10^{-2}$	$0.5{\cdot}10^{-2}$
Diagonal arithmetic mean	$2.7{\cdot}10^{-4}$	-	$1.8{\cdot}10^{-2}$	-
Maximum diagonal	$2.7{\cdot}10^{-4}$	-	$1.8{\cdot}10^{-2}$	-
Minimum diagonal	$2.7{\cdot}10^{-4}$	-	$1.8{\cdot}10^{-2}$	-

Figure 3.11: Error depending on element size measure.

These results show that the best element size measure in the analyzed problem, that is, the element size measure that leads to the lowest error, is the minimum side. On the contrary, the measure that generates the biggest error is the maximum side. Note that this result holds for quadrilateral and triangular elements. This table has been obtained using a uniform mesh but the results with a non-uniform one follow the same pattern. In conclusion,

it is important to remind that the measure of the element size plays an important role in the accuracy of the solution obtained.

3.1.2 Cavity flow problem

The Cavity flow problem has become a standard test for incompressible flows. This problem represents a plane flow in a square cavity. The upper side of the cavity moves at unit speed while the other ones are fixed. The boundary conditions in this problem are drawn in figure 3.12:

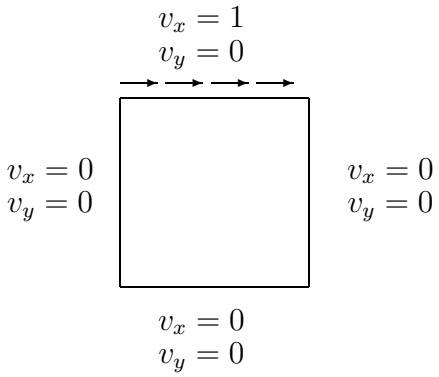

Figure 3.12: Boundary conditions of the Cavity flow problem

It is well known that quadratic elements produce more accurate solutions than linear elements. Moreover, quadratic elements pass the LBB condition. Therefore, the obtained solution using a fine mesh of quadratic elements can be considered as a reference solution, see figure 3.13. Thus, the solutions obtained with linear elements will be compared to the reference solution.

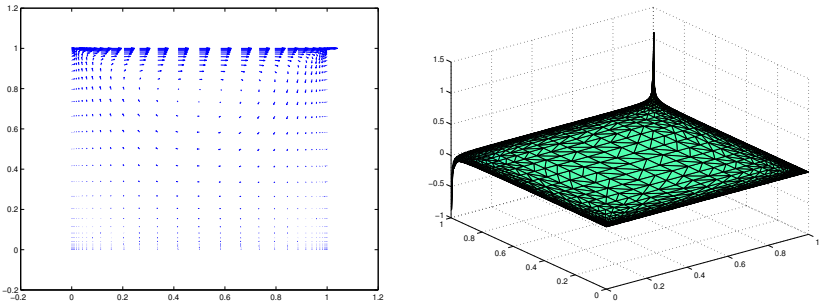

(a) Velocity field (b) Pressure field

Figure 3.13: Solution of the Cavity flow problem obtained with a mesh of 20x20 non-uniform quadratic quadrilateral elements

Comparison between stabilized and non-stabilized solution

The cavity flow problem has been solved using the two types of elements implemented in this work, that is, quadrilateral and triangular elements. The meshes used are non-uniform distributed, as shown in figure 3.14.

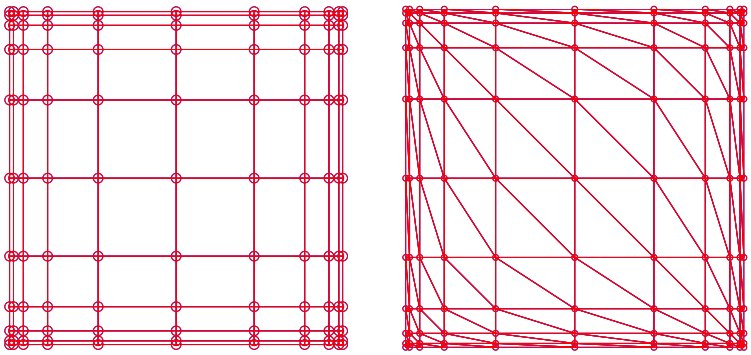

(a) Non-uniform quadrilateral (b) Non-uniform triangular

Figure 3.14: Type of non-uniform meshes used to solve the cavity flow problem.

Figure 3.15 illustrates the behavior of the solution when using 40x40 non-uniform distributed linear quadrilateral elements with and without the stabilization method GLS. Note that the pressure field obtained without using the stabilization method presents big instabilities in the corners of the domain, see figure 3.15(b). On the contrary, the stabilized solution reproduces the reference solution, both for the velocity and pressure fields, see figure 3.15(d). The same analysis is valid for solving the problem using a mesh with triangular elements, see figure 3.16.

Note that these results have been obtained with a non-uniform mesh. This type of mesh is better in this case because it concentrates the elements where the velocity and pressure gradients are higher. This results in a better approximation to the solution.

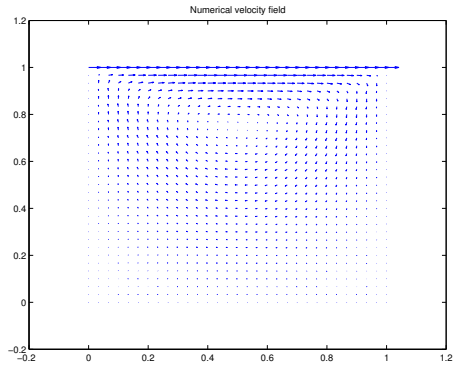

(a) Velocity field without GLS

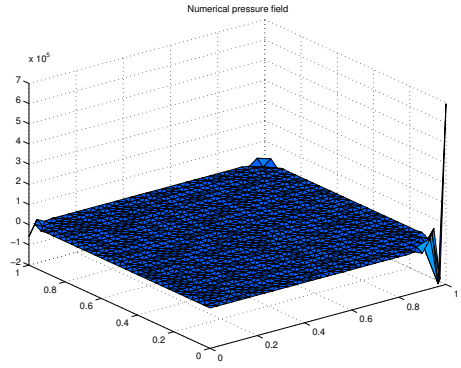

(b) Pressure field without GLS

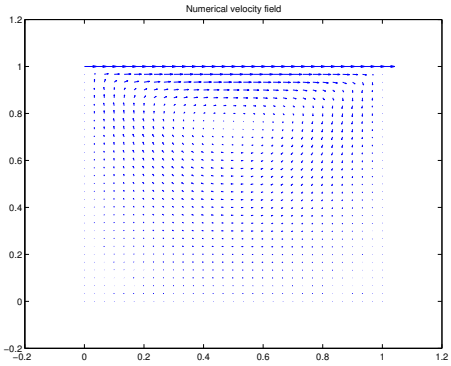

(c) Velocity field with GLS

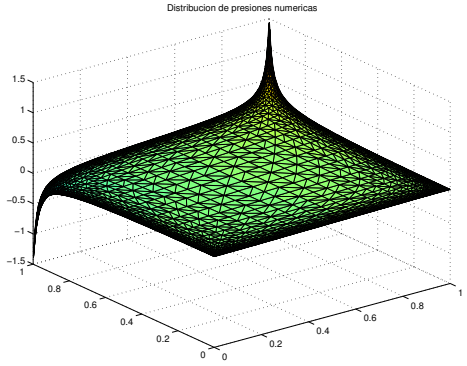

(d) Pressure field with GLS

Figure 3.15: Comparison between stabilized and non-stabilized solution using quadrilateral elements

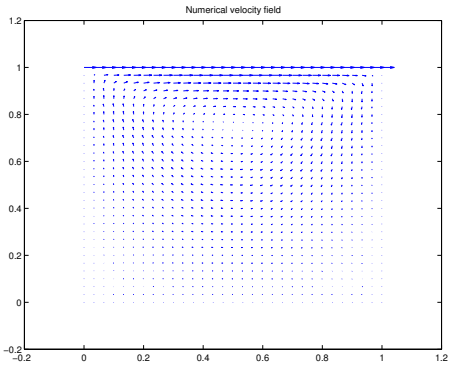

(a) Velocity field without GLS

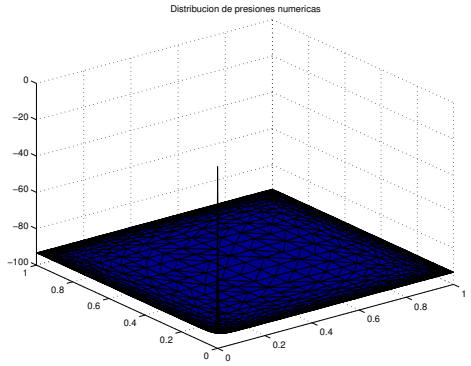

(b) Pressure field without GLS

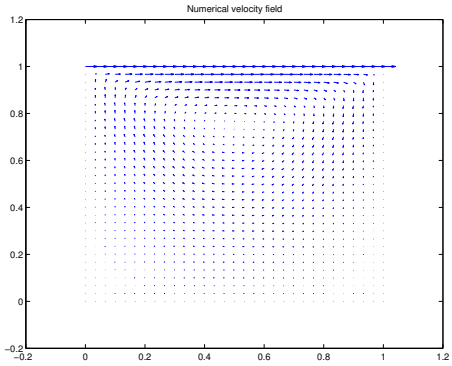

(c) Velocity field with GLS

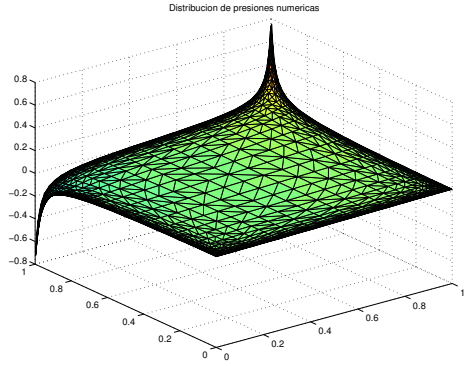

(d) Pressure field with GLS

Figure 3.16: Comparison between stabilized and non-stabilized solution using triangular elements

3.2 Tridimensional case

The numerical solution to the stationary Stokes problem in three dimensions follows the same patterns than in two dimensions. The type of elements used in this case are the generalization of the elements presented in two dimensions. That is, hexahedral and tetrahedral elements. The different kind of elements used for the tridimensional analysis are shown in figure 3.17.

It is also important to define the node numeration in every type of element in order to implement the finite element method properly. The elements implemented in this work are: the bilinear hexahedral (8 nodes), two quadratic hexahedral (20 and 27 nodes) and a linear tetrahedral (4 nodes). The node numeration of every element type is presented in figure 3.18.

The integrals are calculated using a Gauss quadrature as in the bidimensional case. The values of the Gauss points coordinates and their correspondent weights are shown in figure 3.19. Finally, the shape functions are presented in figure 3.20.

Mixed elements			
Figure	Name	Velocity interpolation	Pressure interpolation
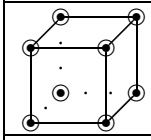	H1H1	Linear	Linear
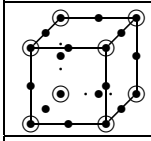	H2H1 (20 nodes)	Quadratic	Linear
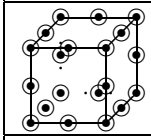	H2H2 (20 nodes)	Quadratic	Quadratic
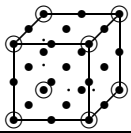	H2H1 (27 nodes)	Quadratic	Linear
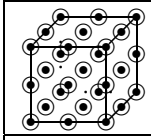	H2H2 (27 nodes)	Quadratic	Quadratic
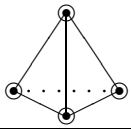	T1T1	Linear	Linear
• Velocity node ○ Pressure node			

Figure 3.17: Types of mixed elements in 3 dimensions

Node numeration	Type of element
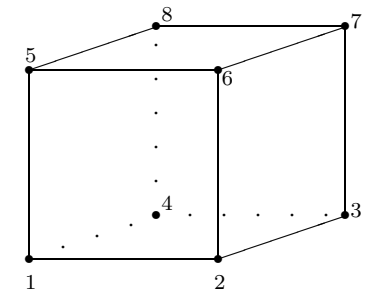	Linear Hexahedral
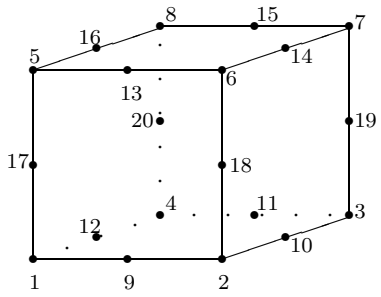	Quadratic Hexahedral (20 nodes)
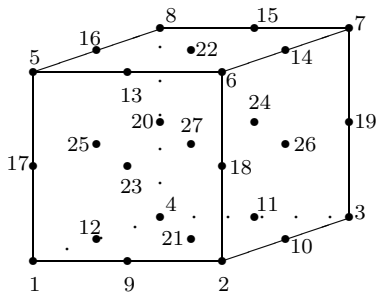	Quadratic Hexahedral (27 nodes)
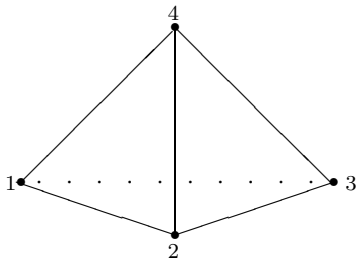	Linear Tetrahedral

Figure 3.18: Node numeration in 3D elements

Element type	Approximation	Gauss points	Gauss weights
Hexahedral	Linear	(-.577350,-.577350,-.577350)	1.000000
		(.577350,-.577350,-.577350)	1.000000
		(-.577350,.577350,-.577350)	1.000000
		(.577350,.577350,-.577350)	1.000000
		(-.577350,-.577350,.577350)	1.000000
		(.577350,-.577350,.577350)	1.000000
		(-.577350,.577350,.577350)	1.000000
		(.577350,.577350,.577350)	1.000000
	Quadratic	(-.774597,-.774597,-.774597)	.171468
		(0,-.774597,-.774597)	.274348
		(.774597,-.774597,-.774597)	.171468
		(-.774597,0,-.774597)	.274348
		(0,0,-.774597)	.438957
		(.774597,0,-.774597)	.274348
		(-.774597,.774597,-.774597)	.171468
		(0,.774597,-.774597)	.274348
		(.774597,.774597,-.774597)	.171468
		(-.774597,-.774597,0)	.274348
		(0,-.774597,0)	.438957
		(.774597,-.774597,0)	.274348
		(-.774597,0,0)	.438957
		(0,0,0)	.702332
		(.774597,0,0)	.438957
		(-.774597,.774597,0)	.274348
		(0,.774597,0)	.438957
		(.774597,.774597,0)	.274348
		(-.774597,-.774597,.774597)	.171468
		(0,-.774597,.774597)	.274348
		(.774597,-.774597,.774597)	.171468
		(-.774597,0,.774597)	.274348
		(0,0,.774597)	.438957
		(.774597,0,.774597)	.274348
		(-.774597,.774597,.774597)	.171468
		(0,.774597,.774597)	.274348
		(.774597,.774597,.774597)	.171468
Tetrahedral	Linear	(.585410,.138197,.138197)	.015625
		(.138197,.585410,.138197)	.015625
		(.138197,.138197,.585410)	.015625
		(.138197,.138197,.138197)	.015625

Figure 3.19: Gauss Quadrature in 3 dimensions

Element type	Approximation	Shape functions
Hexahedral	Linear	$N_1=\frac{1}{8}(1-\xi)(1-\eta)(1-\phi)$ $N_2=\frac{1}{8}(1-\xi)(1+\eta)(1-\phi)$ $N_3=\frac{1}{8}(1+\xi)(1+\eta)(1-\phi)$ $N_4=\frac{1}{8}(1+\xi)(1-\eta)(1-\phi)$ $N_5=\frac{1}{8}(1-\xi)(1-\eta)(1+\phi)$ $N_6=\frac{1}{8}(1-\xi)(1+\eta)(1+\phi)$ $N_7=\frac{1}{8}(1+\xi)(1+\eta)(1+\phi)$ $N_8=\frac{1}{8}(1+\xi)(1-\eta)(1+\phi)$
	Quadratic (20 nodes)	$N_1=\frac{1}{8}(1-\xi)(1-\eta)(1-\phi)(-\xi-\eta-\phi-2)$ $N_2=\frac{1}{8}(1-\xi)(1+\eta)(1-\phi)(-\xi+\eta-\phi-2)$ $N_3=\frac{1}{8}(1+\xi)(1+\eta)(1-\phi)(\xi+\eta-\phi-2)$ $N_4=\frac{1}{8}(1+\xi)(1-\eta)(1-\phi)(\xi-\eta-\phi-2)$ $N_5=\frac{1}{8}(1-\xi)(1-\eta)(1+\phi)(-\xi-\eta+\phi-2)$ $N_6=\frac{1}{8}(1-\xi)(1+\eta)(1+\phi)(-\xi+\eta+\phi-2)$ $N_7=\frac{1}{8}(1+\xi)(1+\eta)(1+\phi)(\xi+\eta+\phi-2)$ $N_8=\frac{1}{8}(1+\xi)(1-\eta)(1+\phi)(\xi-\eta+\phi-2)$ $N_9=\frac{1}{4}(1-\xi^2)(1-\eta)(1-\phi)$ $N_{10}=\frac{1}{4}(1-\eta^2)(1+\xi)(1-\phi)$ $N_{11}=\frac{1}{4}(1-\xi^2)(1+\eta)(1-\phi)$ $N_{12}=\frac{1}{4}(1-\eta^2)(1-\xi)(1-\phi)$ $N_{13}=\frac{1}{4}(1-\phi^2)(1-\eta)(1-\xi)$ $N_{14}=\frac{1}{4}(1-\phi^2)(1-\eta)(1+\xi)$ $N_{15}=\frac{1}{4}(1-\phi^2)(1+\eta)(1+\xi)$ $N_{16}=\frac{1}{4}(1-\phi^2)(1+\eta)(1+\xi)$ $N_{17}=\frac{1}{4}(1-\xi^2)(1-\eta)(1+\phi)$ $N_{18}=\frac{1}{4}(1-\eta^2)(1+\xi)(1+\phi)$ $N_{19}=\frac{1}{4}(1-\xi^2)(1+\eta)(1+\phi)$ $N_{20}=\frac{1}{4}(1-\eta^2)(1-\xi)(1+\phi)$
	Quadratic (27 nodes)	$N_1=\frac{1}{8}\xi(\xi-1)\eta(\eta-1)\phi(\phi-1)$ $N_2=\frac{1}{8}\xi(\xi+1)\eta(\eta-1)\phi(\phi-1)$ $N_3=\frac{1}{8}\xi(\xi+1)\eta(\eta+1)\phi(\phi-1)$ $N_4=\frac{1}{8}\xi(\xi-1)\eta(\eta+1)\phi(\phi-1)$ $N_5=\frac{1}{8}\xi(\xi-1)\eta(\eta-1)\phi(\phi+1)$ $N_6=\frac{1}{8}\xi(\xi+1)\eta(\eta-1)\phi(\phi+1)$ $N_7=\frac{1}{8}\xi(\xi+1)\eta(\eta+1)\phi(\phi+1)$ $N_8=\frac{1}{8}\xi(\xi-1)\eta(\eta+1)\phi(\phi+1)$ $N_9=\frac{1}{4}(1-\xi^2)\eta(\eta-1)\phi(\phi-1)$ $N_{10}=\frac{1}{4}(1-\eta^2)\xi(\xi+1)\phi(\phi-1)$

Hexahedral	Quadratic (27 nodes)	$N_{11}=\frac{1}{4}(1-\xi^2)\eta(\eta+1)\phi(\phi-1)$ $N_{12}=\frac{1}{4}(1-\eta^2)\xi(\xi-1)\phi(\phi-1)$ $N_{13}=\frac{1}{4}(1-\xi^2)\eta(\eta-1)\phi(\phi+1)$ $N_{14}=\frac{1}{4}(1-\eta^2)\xi(\xi+1)\phi(\phi+1)$ $N_{15}=\frac{1}{4}(1-\xi^2)\eta(\eta+1)\phi(\phi+1)$ $N_{16}=\frac{1}{4}(1-\eta^2)\xi(\xi-1)\phi(\phi+1)$ $N_{17}=\frac{1}{4}\xi(\xi-1)\eta(\eta-1)(1-\phi^2)$ $N_{18}=\frac{1}{4}\xi(\xi+1)\eta(\eta-1)(1-\phi^2)$ $N_{19}=\frac{1}{4}\xi(\xi+1)\eta(\eta+1)(1-\phi^2)$ $N_{20}=\frac{1}{4}\xi(\xi-1)\eta(\eta+1)(1-\phi^2)$ $N_{21}=\frac{1}{2}(1-\xi^2)(1-\eta^2)\phi(\phi-1)$ $N_{22}=\frac{1}{2}(1-\xi^2)(1-\eta^2)\phi(\phi+1)$ $N_{23}=\frac{1}{2}(1-\xi^2)\eta(\eta-1)(1-\phi^2)$ $N_{24}=\frac{1}{2}(1-\eta^2)\xi(\xi+1)(1-\phi^2)$ $N_{25}=\frac{1}{2}(1-\xi^2)\eta(\eta+1)(1-\phi^2)$ $N_{26}=\frac{1}{2}(1-\eta^2)\xi(\xi-1)(1-\phi^2)$ $N_{27}=(1-\xi^2)(1-\eta^2)(1-\phi^2)$
Tetrahedral	Linear	$N_1=1$ $N_2=0$ $N_3=0$ $N_4=-1$

Figure 3.20: Shape functions in 3 dimensions

3.2.1 Problem with analytical solution

There are also several Stokes problems with analytical solution in three dimensions. The velocity field has also to verify the incompressibility condition, $\boldsymbol{\nabla v} = 0$. A suitable analytical velocity field can be found extending the analytical field presented for the bidimensional case to the three dimensional one. Hence, the analytical velocity field in three dimensions is chosen as,

$$\begin{aligned} v_1(x,y,z) &= x^2(1-x)^2(2y-6y^2+4y^3)(2z-6z^2+4z^3) \\ v_2(x,y,z) &= y^2(1-y)^2(2x-6x^2+4x^3)(2z-6z^2+4z^3) \\ v_3(x,y,z) &= -2z^2(1-z)^2(2x-6x^2+4x^3)(2y-6y^2+4y^3) \end{aligned}$$

The viscosity is taken as 1 whereas the pressure field has only to be continue because it is just needed its gradient, see (2.12). The pressure field chosen in this work is,

$$p(x,y,z) = x^2 + y^2 + z^2$$

Then, according to equation (2.12) the components of the body forces are,

$$\begin{aligned} b_1 = \; & -(x^4-2x^3+x^2)\big[(2y-6y^2+4y^3)(-12+24z)+(2z-6z^2+4z^3) \\ & (-12+24y)\big]+(2z-6z^2+4z^3)(2y-6y^2+4y^3)(2-12x+12x^2)+2x \\ b_2 = \; & -(y^4-2y^3+y^2)\big[(2x-6x^2+4x^3)(-12+24z)+(2z-6z^2+4z^3) \\ & (-12+24x)\big]+(2z-6z^2+4z^3)(2x-6x^2+4x^3)(2-12y+12y^2)+2y \\ b_3 = \; & 2(z^4-2z^3+z^2)\big[(2y-6y^2+4y^3)(-12+24x)+(2x-6x^2+4x^3) \\ & (-12+24y)\big]+2(2x-6x^2+4x^3)(2y-6y^2+4y^3)(2-12z+12z^2)+2z \end{aligned}$$

The computational domain in this case is a cube, $\Omega = [0,1] \times [0,1] \times [0,1]$. Similar to the two dimensional example, there are several kinds of discretization for the three dimensional domain. Figure 3.21 shows four discretizations. Figures 3.21(a) and 3.21(b) show the meshes with hexahedral elements, uniform and non-uniform distributed, respectively. Similarly, figures 3.21(c) and 3.21(d) display two meshes composed by tetrahedral elements, with an uniform and a non-uniform distribution of the elements, respectively. In these cases, the mesh is composed by 5 elements in each dimension in order to see clearly the resulting mesh. Note that, as in the bidimensional case, the tetrahedral elements in the corners are modified to avoid elements with all nodes being belonging to the boundary.

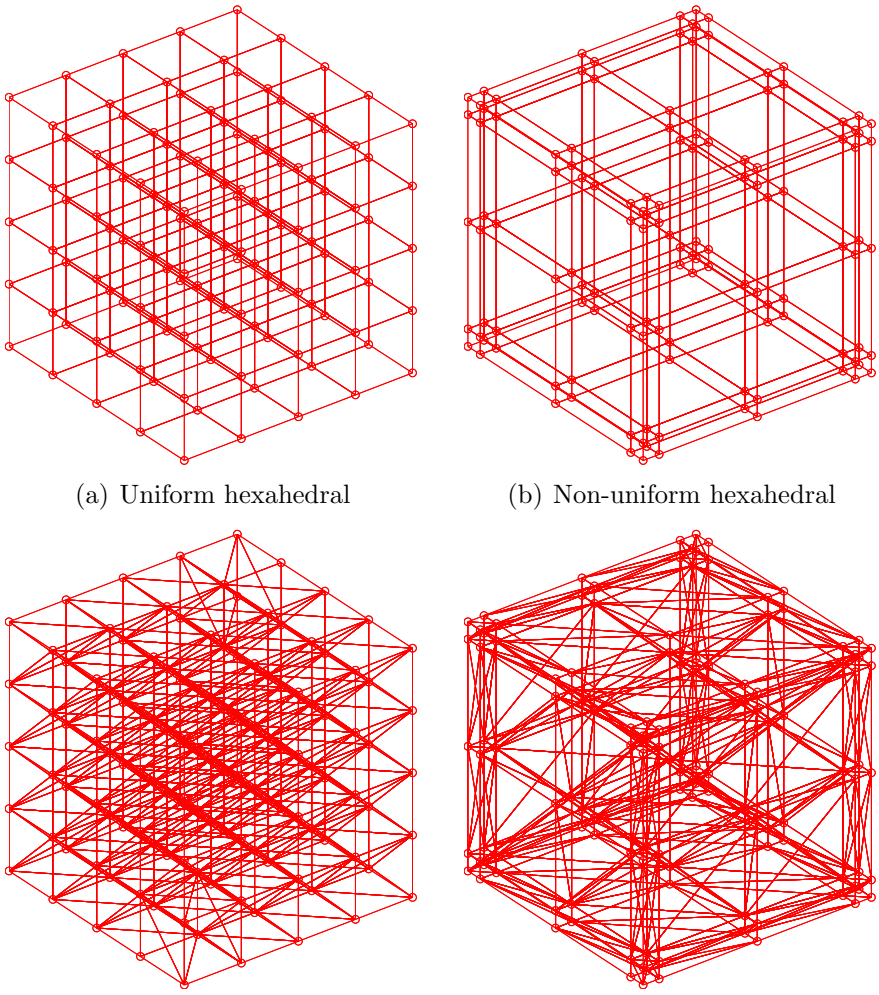

(a) Uniform hexahedral

(b) Non-uniform hexahedral

(c) Uniform tetrahedral

(d) Non-uniform tetrahedral

Figure 3.21: Type of 3D meshes

Comparison between stabilized and non-stabilized solution

In order to analyze the numerical solution obtained by the Galerkin Least-Squares method, figures from figure 3.22 to figure 3.25, show the computed velocity and pressure fields using a mesh composed by 10x10x10 linear hexahedral elements. The use of the stabilization method becomes critical in order to have an acceptable solution to the problem. In particular, figure 3.22(a) represents the horizontal components of the velocity field in the plane z = 0.3 of the solution obtained without implementing the stabilization method. Similarly, figure 3.22(b) shows the component v_z of the velocity field in the same plane z = 0.3. These graphics clearly indicate that the obtained solution is unacceptable due to the instabilities appeared. On the contrary, figures 3.23(a) and 3.23(b) display the solution obtained implementing the stabilization method. In this case, the solution can be accepted in comparison to the analytical solution.

The analysis of the pressure field is analog to the analysis of the velocity field. Figure 3.24 displays the pressure field in the plane z = 0.3 of the solution obtained without using the stabilization method. Similarly, figure 3.25 shows the pressure field in the plane z = 0.3 obtained with the implementation of the stabilization method. The differences between the behavior of the non-stabilized and the stabilized numerical solution can be clearly observed. The non-stabilized solution is unacceptable whereas the stabilized solution reflects the same behavior as the analytical solution.

Both the non-stabilized and the stabilized solutions have been shown at plane z = 0.3 as an example. The behavior of the solutions in the other planes, from z = 0 to z = 1 is analog to the behavior in plane z = 0.3. Moreover, the solution obtained with meshes of tetrahedral elements follow the same pattern than the behavior shown in meshes with hexahedral elements.

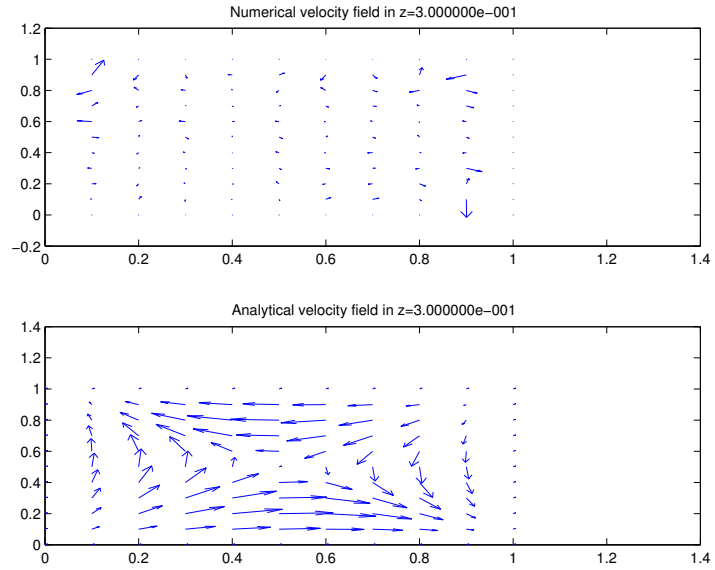

(a)

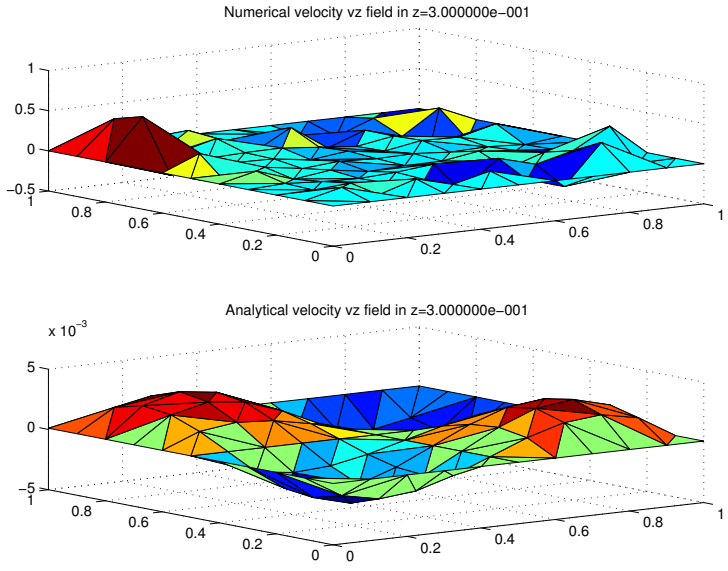

(b)

Figure 3.22: Velocity field of the non-stabilized solution

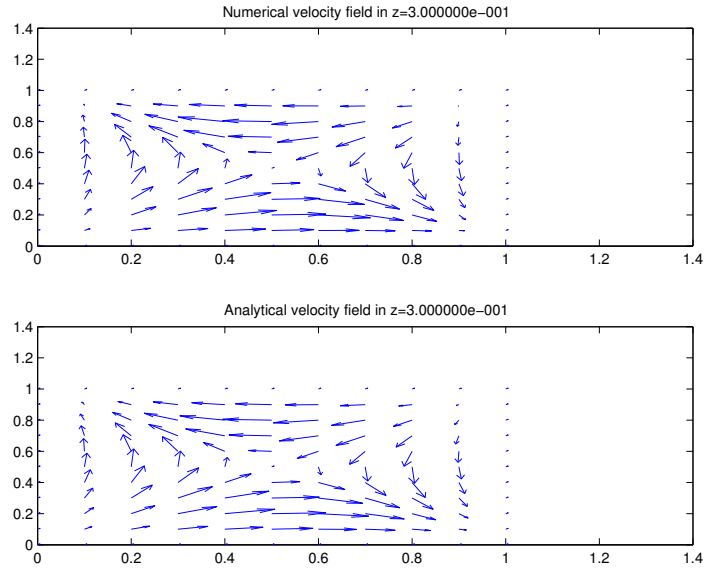

(a)

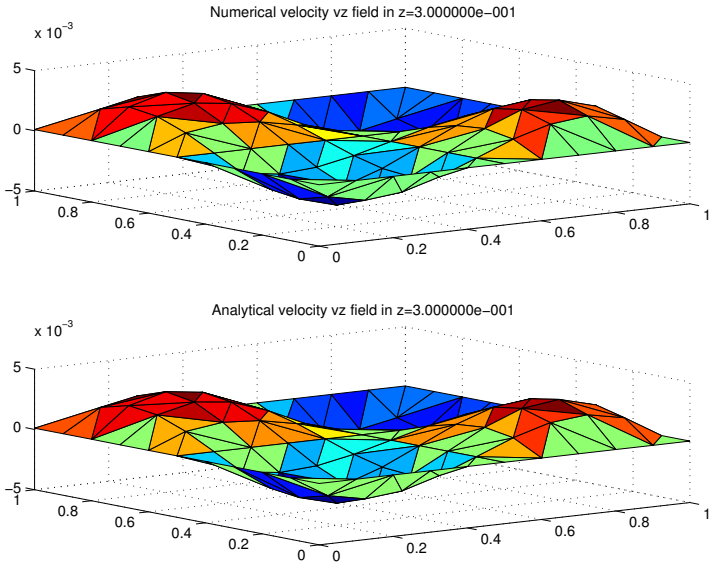

(b)

Figure 3.23: Velocity field of the stabilized solution

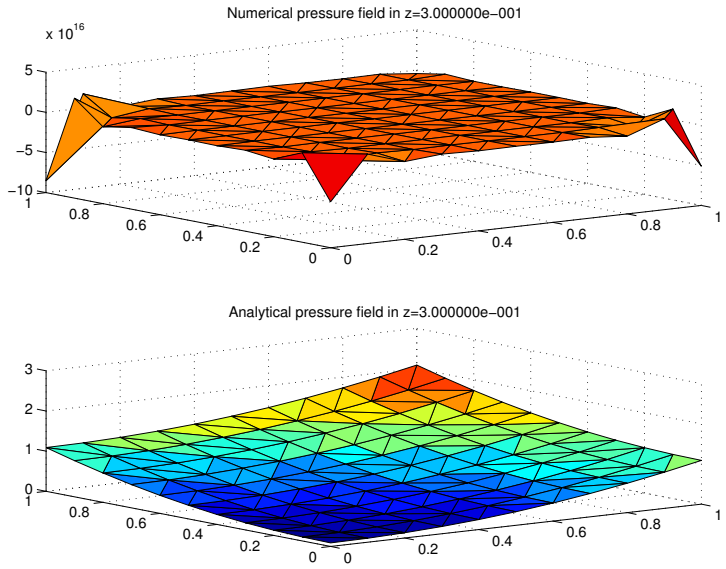

(a)

Figure 3.24: Pressure field of the non-stabilized solution

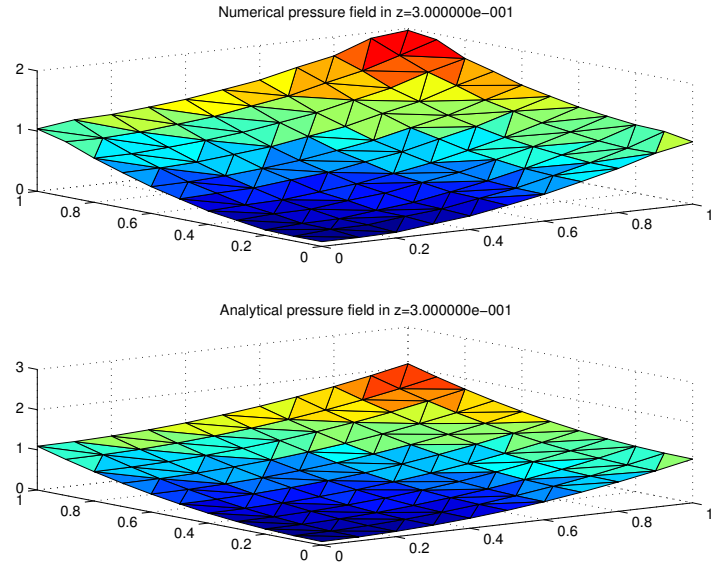

(a)

Figure 3.25: Pressure field of the stabilized solution

Error depending on the stabilization parameter

The accuracy of the stabilization method can be evaluated comparing the analytical and the numerical solution of the stationary Stokes problem in three dimensions. From the theoretical point of view, the behavior of the errors should be similar to the obtained in the two dimension case. That is, the stabilization parameter should only depend on the element size measure. However, the results obtained in this work show no clear relation in this issue. Therefore, the study has to be extended to find other variables that may influence on the numerical solution.

The other variable in the stabilization parameter is the viscosity. A deeper study focusing in the viscosity allows a better knowledge of the stationary Stokes problem. Figures from 3.26 to 3.29 show the errors of the velocity and pressure fields obtained for different values of the viscosity. These errors have been computed solving the stationary Stokes problem with analytical solution in three dimensions in a mesh of linear hexahedral elements using the Galerkin Least-Squares method. The obtained results lead to the conclusion that the stabilization parameter has to be multiplied by a constant depending on the viscosity of the fluid studied, at least for these coarse meshes. This implies a new definition of the stabilization parameter, see (2.54)

$$\tau_e = \alpha_0 \frac{h_e^2}{4C\nu} \tag{3.3}$$

where C is a constant value.

In particular, figure 3.26 presents a table with the errors obtained solving the stationary Stokes problem in a fluid with viscosity $\nu = 10$. The numerical solution is obtained for several structured meshes that range from 11x11x11 elements to 19x19x19 elements. As it can be observed, the error in the pressure and the velocity fields decreases as C goes from $C = 1$ to $C = 100$. However, for $C = 1000$ and $C = 10000$ the error raises to unacceptable values. Figure 3.27 shows the error of the numerical solution for a fluid with viscosity $\nu = 1$. In this case, the pressure error decreases as C raises from $C = 1$ to $C = 10000$. However, the velocity error values reach a minimum for $C = 100$ and increase for higher values of C. The behavior of fluids with viscosities of $\nu = 0.1$ and $\nu = 0.01$ is similar to a fluid with viscosity $\nu = 1$, see figures 3.28 and 3.29. As it can be seen, the pressure error is reduced when the constant applied to the stabilization parameter C increases. The velocity errors also decrease when the constant raises until $C = 1000$ and

$C = 10000$, respectively.

Figure 3.30 shows the error results versus the constant applied to the stabilization parameter depending on the viscosity fluid. These graphics are obtained solving the stationary Stokes problem in a mesh of 19x19x19 linear hexahedral elements. In particular, figure 3.30(a) represents the maximum absolute error of the horizontal components of the velocity field in logarithmical axes, and figure 3.30(b) the error of the z-component of the velocity field in logarithmical axes, too. Figure 3.30(c) shows the error of the pressure field in semilogarithmical axes. These figures clearly represent the behavior of the solution. The velocity errors are reduced when high values of the constant C are used. Moreover, this behavior does not depend on the viscosity of the fluid. However, as the viscosity of the fluid decreases, higher values of C are needed in order to obtain an acceptable solution. The pressure error is also reduced as long as the constant applied is augmented except in the case of a fluid with viscosity of $\nu = 10$. In this case, the pressure error is minimum for a constant of $C = 100$.

In conclusion, the stability of the solution of the stationary Stokes problem using a finite element method with the stabilization method Galerkin Least-Squares depends critically on the viscosity of the fluid. The stabilization parameter has to be modified by a constant that varies depending on the viscosity value.

Viscosity ν = 10				
C=1				
Elements	Error P	Error Vx	Error Vy	Error Vz
11x11x11	0.7554	$5.54{\cdot}10^{-4}$	$5.54{\cdot}10^{-4}$	$5.64{\cdot}10^{-4}$
13x13x13	0.6539	$4.35{\cdot}10^{-4}$	$4.35{\cdot}10^{-4}$	$4.58{\cdot}10^{-4}$
15x15x15	0.5762	$3.58{\cdot}10^{-4}$	$3.58{\cdot}10^{-4}$	$3.75{\cdot}10^{-4}$
17x17x17	0.5149	$3.05{\cdot}10^{-4}$	$3.05{\cdot}10^{-4}$	$3.17{\cdot}10^{-4}$
19x19x19	0.4653	$2.67{\cdot}10^{-4}$	$2.67{\cdot}10^{-4}$	$2.76{\cdot}10^{-4}$
C=10				
Elements	Error P	Error Vx	Error Vy	Error Vz
11x11x11	0.3471	$2.19{\cdot}10^{-4}$	$2.19{\cdot}10^{-4}$	$2.82{\cdot}10^{-4}$
13x13x13	0.2970	$1.89{\cdot}10^{-4}$	$1.89{\cdot}10^{-4}$	$2.46{\cdot}10^{-4}$
15x15x15	0.2595	$1.66{\cdot}10^{-4}$	$1.66{\cdot}10^{-4}$	$2.12{\cdot}10^{-4}$
17x17x17	0.2304	$1.53{\cdot}10^{-4}$	$1.53{\cdot}10^{-4}$	$1.87{\cdot}10^{-4}$
19x19x19	0.2071	$1.43{\cdot}10^{-4}$	$1.43{\cdot}10^{-4}$	$1.70{\cdot}10^{-4}$
C=100				
Elements	Error P	Error Vx	Error Vy	Error Vz
11x11x11	0.2798	$2.39{\cdot}10^{-4}$	$2.39{\cdot}10^{-4}$	$3.19{\cdot}10^{-4}$
13x13x13	0.2492	$1.99{\cdot}10^{-4}$	$1.99{\cdot}10^{-4}$	$2.57{\cdot}10^{-4}$
15x15x15	0.2145	$1.69{\cdot}10^{-4}$	$1.69{\cdot}10^{-4}$	$2.04{\cdot}10^{-4}$
17x17x17	0.1810	$1.51{\cdot}10^{-4}$	$1.51{\cdot}10^{-4}$	$1.84{\cdot}10^{-4}$
19x19x19	0.1520	$1.40{\cdot}10^{-4}$	$1.40{\cdot}10^{-4}$	$1.68{\cdot}10^{-4}$
C=1000				
Elements	Error P	Error Vx	Error Vy	Error Vz
11x11x11	0.8028	$3.29{\cdot}10^{-4}$	$3.29{\cdot}10^{-4}$	$3.60{\cdot}10^{-4}$
13x13x13	0.7035	$2.56{\cdot}10^{-4}$	$2.56{\cdot}10^{-4}$	$2.88{\cdot}10^{-4}$
15x15x15	0.6241	$2.05{\cdot}10^{-4}$	$2.05{\cdot}10^{-4}$	$2.25{\cdot}10^{-4}$
17x17x17	0.5577	$1.79{\cdot}10^{-4}$	$1.79{\cdot}10^{-4}$	$1.98{\cdot}10^{-4}$
19x19x19	0.4996	$1.61{\cdot}10^{-4}$	$1.61{\cdot}10^{-4}$	$1.79{\cdot}10^{-4}$
C=10000				
Elements	Error P	Error Vx	Error Vy	Error Vz
11x11x11	0.9911	$3.57{\cdot}10^{-4}$	$3.57{\cdot}10^{-4}$	$3.74{\cdot}10^{-4}$
13x13x13	0.9232	$2.81{\cdot}10^{-4}$	$2.81{\cdot}10^{-4}$	$3.00{\cdot}10^{-4}$
15x15x15	0.8786	$2.27{\cdot}10^{-4}$	$2.27{\cdot}10^{-4}$	$2.35{\cdot}10^{-4}$
17x17x17	0.8450	$1.96{\cdot}10^{-4}$	$1.96{\cdot}10^{-4}$	$2.06{\cdot}10^{-4}$
19x19x19	0.8237	$1.76{\cdot}10^{-4}$	$1.76{\cdot}10^{-4}$	$1.85{\cdot}10^{-4}$

Figure 3.26: **Errors for viscosity ν = 10**

Viscosity $\nu = 1$				
C=1				
Elements	Error P	Error Vx	Error Vy	Error Vz
11x11x11	0.7554	$4.30{\cdot}10^{-3}$	$4.30{\cdot}10^{-3}$	$4.26{\cdot}10^{-3}$
13x13x13	0.6539	$3.40{\cdot}10^{-3}$	$3.40{\cdot}10^{-3}$	$3.39{\cdot}10^{-3}$
15x15x15	0.5762	$2.66{\cdot}10^{-3}$	$2.66{\cdot}10^{-3}$	$2.67{\cdot}10^{-3}$
17x17x17	0.5149	$2.15{\cdot}10^{-3}$	$2.15{\cdot}10^{-3}$	$2.16{\cdot}10^{-3}$
19x19x19	0.4653	$1.77{\cdot}10^{-3}$	$1.77{\cdot}10^{-3}$	$1.79{\cdot}10^{-3}$
C=10				
Elements	Error P	Error Vx	Error Vy	Error Vz
11x11x11	0.3471	$1.04{\cdot}10^{-3}$	$1.04{\cdot}10^{-3}$	$1.12{\cdot}10^{-3}$
13x13x13	0.2970	$9.35{\cdot}10^{-4}$	$9.35{\cdot}10^{-4}$	$9.83{\cdot}10^{-4}$
15x15x15	0.2595	$7.40{\cdot}10^{-4}$	$7.40{\cdot}10^{-4}$	$7.69{\cdot}10^{-4}$
17x17x17	0.2304	$6.05{\cdot}10^{-4}$	$6.05{\cdot}10^{-4}$	$6.25{\cdot}10^{-4}$
19x19x19	0.2071	$5.09{\cdot}10^{-4}$	$5.09{\cdot}10^{-4}$	$5.22{\cdot}10^{-4}$
C=100				
Elements	Error P	Error Vx	Error Vy	Error Vz
11x11x11	0.2401	$2.40{\cdot}10^{-4}$	$2.40{\cdot}10^{-4}$	$3.10{\cdot}10^{-4}$
13x13x13	0.2051	$2.20{\cdot}10^{-4}$	$2.20{\cdot}10^{-4}$	$2.76{\cdot}10^{-4}$
15x15x15	0.1790	$1.93{\cdot}10^{-4}$	$1.93{\cdot}10^{-4}$	$2.35{\cdot}10^{-4}$
17x17x17	0.1587	$1.74{\cdot}10^{-4}$	$1.74{\cdot}10^{-4}$	$2.08{\cdot}10^{-4}$
19x19x19	0.1426	$1.59{\cdot}10^{-4}$	$1.59{\cdot}10^{-4}$	$1.88{\cdot}10^{-4}$
C=1000				
Elements	Error P	Error Vx	Error Vy	Error Vz
11x11x11	0.2194	$3.30{\cdot}10^{-4}$	$3.30{\cdot}10^{-4}$	$3.60{\cdot}10^{-4}$
13x13x13	0.1877	$2.58{\cdot}10^{-4}$	$2.58{\cdot}10^{-4}$	$2.89{\cdot}10^{-4}$
15x15x15	0.1639	$2.07{\cdot}10^{-4}$	$2.07{\cdot}10^{-4}$	$2.26{\cdot}10^{-4}$
17x17x17	0.1455	$1.80{\cdot}10^{-4}$	$1.80{\cdot}10^{-4}$	$1.99{\cdot}10^{-4}$
19x19x19	0.1308	$1.62{\cdot}10^{-4}$	$1.62{\cdot}10^{-4}$	$1.80{\cdot}10^{-4}$
C=10000				
Elements	Error P	Error Vx	Error Vy	Error Vz
11x11x11	0.2164	$3.57{\cdot}10^{-4}$	$3.57{\cdot}10^{-4}$	$3.74{\cdot}10^{-4}$
13x13x13	0.1851	$2.81{\cdot}10^{-4}$	$2.81{\cdot}10^{-4}$	$3.00{\cdot}10^{-4}$
15x15x15	0.1617	$2.28{\cdot}10^{-4}$	$2.28{\cdot}10^{-4}$	$2.35{\cdot}10^{-4}$
17x17x17	0.1435	$1.96{\cdot}10^{-4}$	$1.96{\cdot}10^{-4}$	$2.06{\cdot}10^{-4}$
19x19x19	0.1290	$1.75{\cdot}10^{-4}$	$1.75{\cdot}10^{-4}$	$1.86{\cdot}10^{-4}$

Figure 3.27: **Errors for viscosity $\nu = 1$**

Viscosity ν = 0.1				
C=1				
Elements	Error P	Error Vx	Error Vy	Error Vz
11x11x11	0.7554	$4.37{\cdot}10^{-2}$	$4.37{\cdot}10^{-2}$	$4.37{\cdot}10^{-2}$
13x13x13	0.6539	$3.31{\cdot}10^{-2}$	$3.31{\cdot}10^{-2}$	$3.31{\cdot}10^{-2}$
15x15x15	0.5762	$2.58{\cdot}10^{-2}$	$2.58{\cdot}10^{-2}$	$2.58{\cdot}10^{-2}$
17x17x17	0.5149	$2.06{\cdot}10^{-2}$	$2.06{\cdot}10^{-2}$	$2.06{\cdot}10^{-2}$
19x19x19	0.4653	$1.69{\cdot}10^{-3}$	$1.69{\cdot}10^{-2}$	$1.69{\cdot}10^{-2}$
C=10				
Elements	Error P	Error Vx	Error Vy	Error Vz
11x11x11	0.3471	$1.15{\cdot}10^{-2}$	$1.15{\cdot}10^{-2}$	$1.16{\cdot}10^{-2}$
13x13x13	0.2970	$8.59{\cdot}10^{-3}$	$8.59{\cdot}10^{-3}$	$8.64{\cdot}10^{-3}$
15x15x15	0.2595	$6.58{\cdot}10^{-3}$	$6.58{\cdot}10^{-3}$	$6.61{\cdot}10^{-3}$
17x17x17	0.2304	$5.21{\cdot}10^{-3}$	$5.21{\cdot}10^{-3}$	$5.23{\cdot}10^{-3}$
19x19x19	0.2071	$4.23{\cdot}10^{-3}$	$4.23{\cdot}10^{-3}$	$4.24{\cdot}10^{-3}$
C=100				
Elements	Error P	Error Vx	Error Vy	Error Vz
11x11x11	0.2401	$1.61{\cdot}10^{-3}$	$1.61{\cdot}10^{-3}$	$1.70{\cdot}10^{-3}$
13x13x13	0.2051	$1.35{\cdot}10^{-3}$	$1.35{\cdot}10^{-3}$	$1.40{\cdot}10^{-3}$
15x15x15	0.1790	$1.06{\cdot}10^{-3}$	$1.06{\cdot}10^{-3}$	$1.09{\cdot}10^{-3}$
17x17x17	0.1587	$8.59{\cdot}10^{-4}$	$8.59{\cdot}10^{-4}$	$8.73{\cdot}10^{-4}$
19x19x19	0.1426	$7.14{\cdot}10^{-4}$	$7.14{\cdot}10^{-4}$	$7.23{\cdot}10^{-4}$
C=1000				
Elements	Error P	Error Vx	Error Vy	Error Vz
11x11x11	0.2194	$3.40{\cdot}10^{-4}$	$3.40{\cdot}10^{-4}$	$3.59{\cdot}10^{-4}$
13x13x13	0.1877	$2.75{\cdot}10^{-4}$	$2.75{\cdot}10^{-4}$	$3.04{\cdot}10^{-4}$
15x15x15	0.1639	$2.20{\cdot}10^{-4}$	$2.20{\cdot}10^{-4}$	$2.54{\cdot}10^{-4}$
17x17x17	0.1455	$1.93{\cdot}10^{-4}$	$1.93{\cdot}10^{-4}$	$2.17{\cdot}10^{-4}$
19x19x19	0.1308	$1.73{\cdot}10^{-4}$	$1.73{\cdot}10^{-4}$	$1.95{\cdot}10^{-4}$
C=10000				
Elements	Error P	Error Vx	Error Vy	Error Vz
11x11x11	0.2164	$3.59{\cdot}10^{-4}$	$3.59{\cdot}10^{-4}$	$3.74{\cdot}10^{-4}$
13x13x13	0.1851	$2.83{\cdot}10^{-4}$	$2.83{\cdot}10^{-4}$	$3.01{\cdot}10^{-4}$
15x15x15	0.1617	$2.29{\cdot}10^{-4}$	$2.29{\cdot}10^{-4}$	$2.36{\cdot}10^{-4}$
17x17x17	0.1435	$1.97{\cdot}10^{-4}$	$1.97{\cdot}10^{-4}$	$2.08{\cdot}10^{-4}$
19x19x19	0.1290	$1.76{\cdot}10^{-4}$	$1.76{\cdot}10^{-4}$	$1.87{\cdot}10^{-4}$

Figure 3.28: **Errors for viscosity ν = 0.1**

Viscosity ν = 0.01				
C=1				
Elements	Error P	Error Vx	Error Vy	Error Vz
11x11x11	0.7554	$4.38{\cdot}10^{-1}$	$4.38{\cdot}10^{-1}$	$4.38{\cdot}10^{-1}$
13x13x13	0.6539	$3.30{\cdot}10^{-1}$	$3.30{\cdot}10^{-1}$	$3.30{\cdot}10^{-1}$
15x15x15	0.5762	$2.57{\cdot}10^{-1}$	$2.57{\cdot}10^{-1}$	$2.57{\cdot}10^{-1}$
17x17x17	0.5149	$2.05{\cdot}10^{-1}$	$2.05{\cdot}10^{-1}$	$2.05{\cdot}10^{-1}$
19x19x19	0.4653	$1.68{\cdot}10^{-1}$	$1.68{\cdot}10^{-1}$	$1.68{\cdot}10^{-1}$
C=10				
Elements	Error P	Error Vx	Error Vy	Error Vz
11x11x11	0.3471	$1.16{\cdot}10^{-1}$	$1.16{\cdot}10^{-1}$	$1.16{\cdot}10^{-1}$
13x13x13	0.2970	$8.51{\cdot}10^{-2}$	$8.51{\cdot}10^{-2}$	$8.51{\cdot}10^{-2}$
15x15x15	0.2595	$6.49{\cdot}10^{-2}$	$6.49{\cdot}10^{-2}$	$6.50{\cdot}10^{-2}$
17x17x17	0.2304	$5.12{\cdot}10^{-2}$	$5.12{\cdot}10^{-2}$	$5.12{\cdot}10^{-2}$
19x19x19	0.2071	$4.15{\cdot}10^{-2}$	$4.15{\cdot}10^{-2}$	$4.15{\cdot}10^{-2}$
C=100				
Elements	Error P	Error Vx	Error Vy	Error Vz
11x11x11	0.2401	$1.73{\cdot}10^{-2}$	$1.73{\cdot}10^{-2}$	$1.74{\cdot}10^{-2}$
13x13x13	0.2051	$1.28{\cdot}10^{-2}$	$1.28{\cdot}10^{-2}$	$1.29{\cdot}10^{-2}$
15x15x15	0.1790	$9.79{\cdot}10^{-3}$	$9.79{\cdot}10^{-3}$	$9.82{\cdot}10^{-3}$
17x17x17	0.1587	$7.73{\cdot}10^{-3}$	$7.73{\cdot}10^{-3}$	$7.75{\cdot}10^{-3}$
19x19x19	0.1426	$6.27{\cdot}10^{-3}$	$6.27{\cdot}10^{-3}$	$6.28{\cdot}10^{-3}$
C=1000				
Elements	Error P	Error Vx	Error Vy	Error Vz
11x11x11	0.2194	$1.78{\cdot}10^{-3}$	$1.78{\cdot}10^{-3}$	$1.91{\cdot}10^{-3}$
13x13x13	0.1877	$1.48{\cdot}10^{-3}$	$1.48{\cdot}10^{-3}$	$1.55{\cdot}10^{-3}$
15x15x15	0.1639	$1.16{\cdot}10^{-3}$	$1.16{\cdot}10^{-3}$	$1.20{\cdot}10^{-3}$
17x17x17	0.1455	$9.37{\cdot}10^{-4}$	$9.37{\cdot}10^{-4}$	$9.58{\cdot}10^{-4}$
19x19x19	0.1308	$7.77{\cdot}10^{-4}$	$7.77{\cdot}10^{-4}$	$7.89{\cdot}10^{-4}$
C=10000				
Elements	Error P	Error Vx	Error Vy	Error Vz
11x11x11	0.2164	$3.72{\cdot}10^{-4}$	$3.72{\cdot}10^{-4}$	$3.75{\cdot}10^{-4}$
13x13x13	0.1851	$3.01{\cdot}10^{-4}$	$3.01{\cdot}10^{-4}$	$3.13{\cdot}10^{-4}$
15x15x15	0.1617	$2.44{\cdot}10^{-4}$	$2.44{\cdot}10^{-4}$	$2.62{\cdot}10^{-4}$
17x17x17	0.1435	$2.08{\cdot}10^{-4}$	$2.08{\cdot}10^{-4}$	$2.22{\cdot}10^{-4}$
19x19x19	0.1290	$1.87{\cdot}10^{-4}$	$1.87{\cdot}10^{-4}$	$1.98{\cdot}10^{-4}$

Figure 3.29: **Errors for viscosity ν = 0.01**

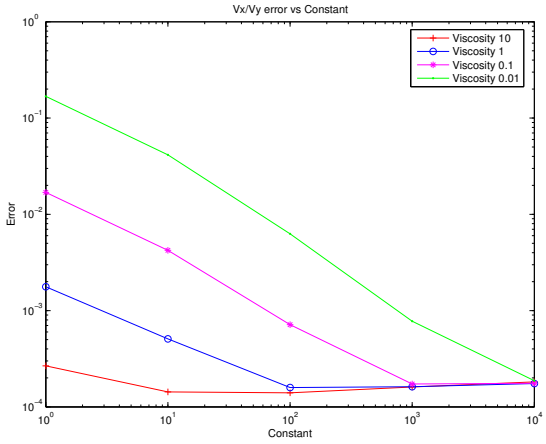

(a)

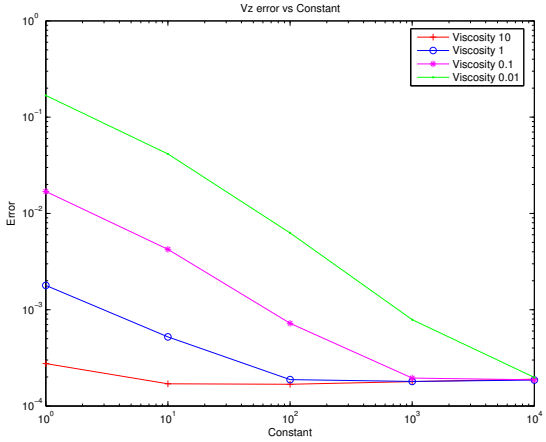

(b)

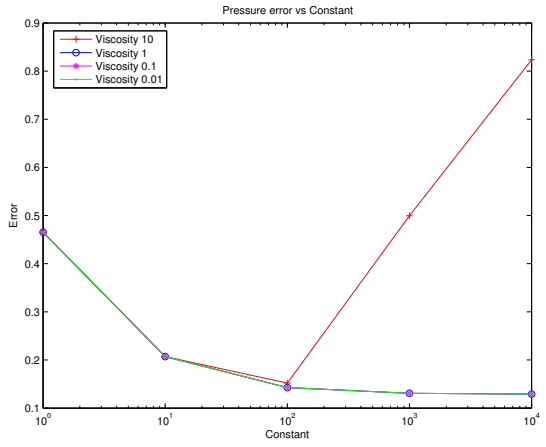

(c)

Figure 3.30: Error vs. Constant depending on the fluid viscosity.

3.2.2 Cavity flow problem

The definition of the Cavity flow problem in three dimensions can be easily derived from the two dimensional case. The domain of the problem is a cubic cavity with unity sides, $\Omega = [0,1] \times [0,1] \times [0,1]$. The upper plane of the cavity moves at unit speed while the other ones are fixed. These boundary conditions can be seen in figure 3.31:

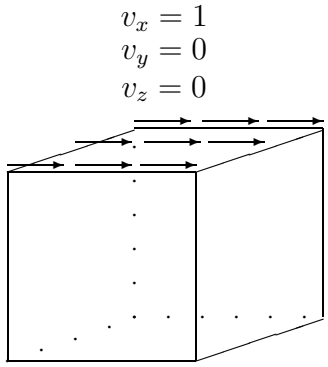

Figure 3.31: Boundary conditions for the Cavity flow problem in 3D

Figures from 3.32 to 3.34 show the numerical solution to the cavity flow problem in three dimensions in a mesh of 20x20x20 linear hexahedral elements with a non-uniform distribution in various planes z. Figures 3.32(a) to 3.34(a) represent the horizontal components of the velocity field. Figures 3.32(b) to 3.34(b) show the z-component of the velocity field. Note that the numerical solution obtained reproduces the boundary conditions of the cavity flow problem, see figures 3.34(a) and 3.34(b). Figures 3.32(c) to 3.34(c) display the pressure field. The behavior of the obtained solution is analog to the two dimensional case. The use of linear elements without the stabilization method leads to an unstable solution. In contrary, the implementation of the Galerkin Least-Squares method enables the use of linear elements obtaining an stable numerical solution.

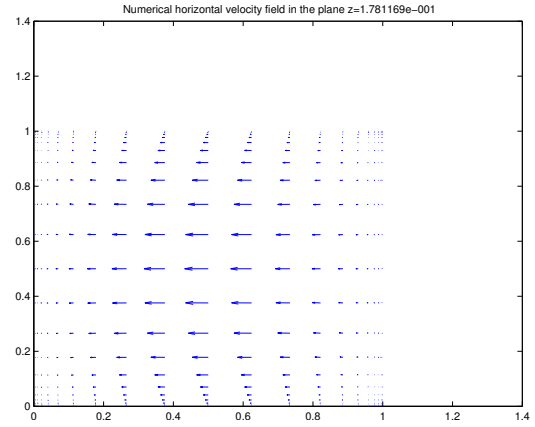

(a)

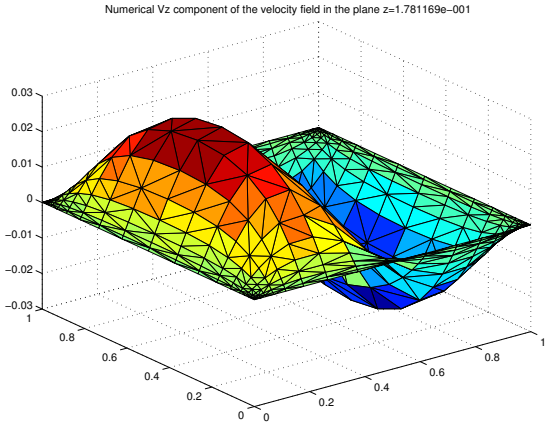

(b)

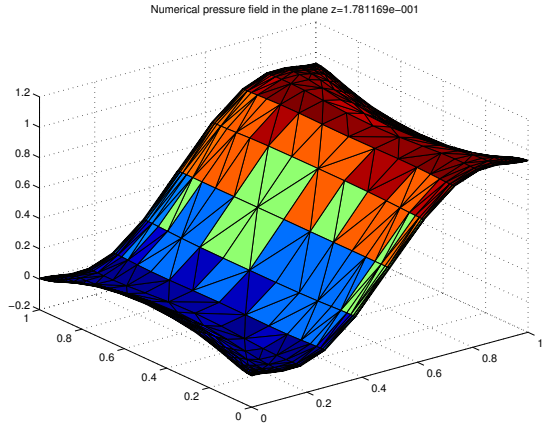

(c)

Figure 3.32: Stabilized solution of the Cavity flow problem in $z = 1.78 \cdot 10^{-1}$

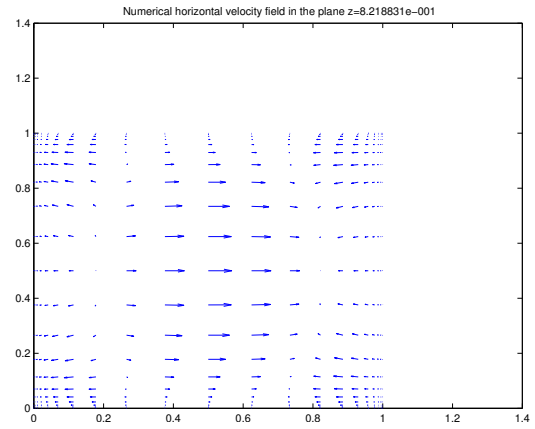

(a)

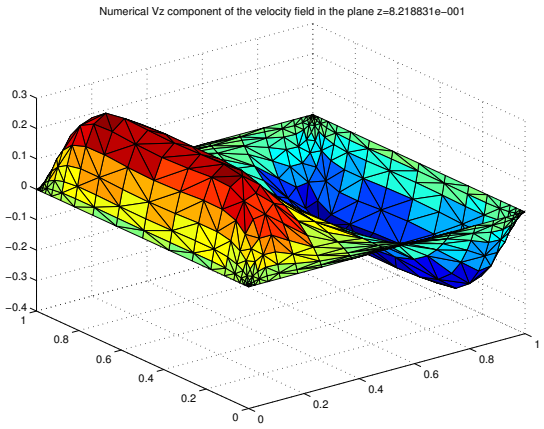

(b)

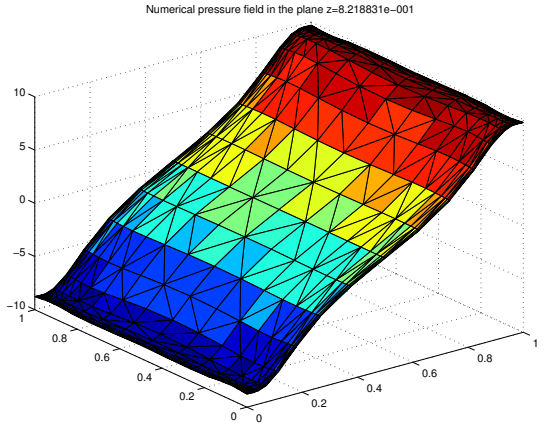

(c)

Figure 3.33: Stabilized solution of the Cavity flow problem in $z = 8.22 \cdot 10^{-1}$

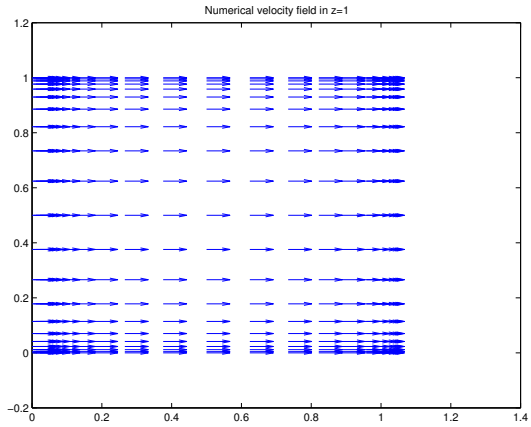

(a)

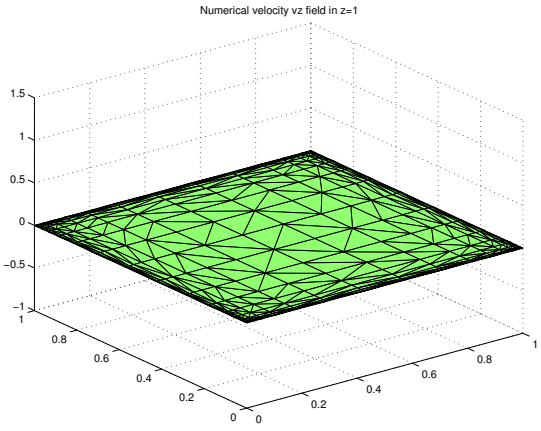

(b)

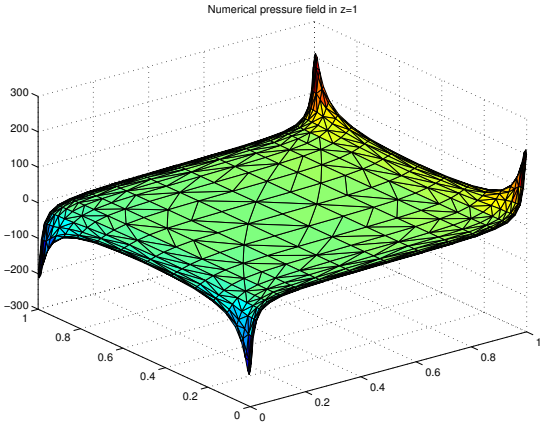

(c)

Figure 3.34: Stabilized solution of the Cavity flow problem in $z = 1.00$